Polymers

CrossMark

Synthesis and characterization of amine-modified spherical nanocellulose aerogels

Xiaoyu Wang[1,2] (iD), Yang Zhang[1,*], Siqun Wang[2,*], Hua Jiang[3], Shuang Liu[1], Yuan Yao[1], Tianmeng Zhang[1], and Qian Li[2]

[1] College of Materials Science and Engineering, Nanjing Forestry University, Nanjing 210037, China
[2] Center for Renewable Carbon, University of Tennessee, Knoxville, TN 37996, USA
[3] College of Chemical Engineering, Nanjing Forestry University, Nanjing 210037, China

ABSTRACT

In this work, cellulose nanocrystal (CNC) was prepared from microcrystalline cellulose (MCC) by acid hydrolysis method. The *N*-(2-aminoethyl)(3-amino-propyl) methyldimethoxysilane (AEAPMDS)-CNC aerogel was successfully fabricated either by freeze-drying or supercritical CO_2 drying of spherical CNC hydrogels into which the amine group has been successfully introduced via C–O–Si bonds between CNC and AEAPMDS. The impact of various parameters (time, temperature, AEAPMDS amount, solid-to-liquid ratio) on the properties of the as-prepared materials is systematically explored, revealing the optimum reaction conditions (100 °C, 16 h, solid-to-liquid ratio of 1:10). The as-prepared spherical nanocellulose aerogels were characterized with respect to textural, structural, thermal and morphological characteristics by various methods (BET, XRD, SEM, TGA, FTIR, and NMR). They exhibited a nano-porous network structure of mesopores possessing a high surface area (262 m^2/g) in the case of supercritical CO_2 drying, whereas a honeycomb structure comprising squares, polygons and circles with a surface area of 120.4 m^2/g was obtained by freeze-drying. The as-synthesized AEAPMDS-CNC aerogels could be potentially applied to capture CO_2 via covalent bonding.

Introduction

With increasing awareness of environmental issues and green technologies, the use of biomaterials instead of petrochemical-based materials is highly desirable [1]. Cellulose, a linear polymer composed of glucose monomer, is recognized as a natural biopolymer which boasts the highest content in the world [2]. It has been extensively explored [3], in terms of its biosynthesis [4], structure analysis [5], chemical modification [6], regeneration of cellulosic materials [7], and applications in various fields.

The use of natural fibers provides several advantages including low density, low cost, adequate mechanical properties and biodegradability [8].

Address correspondence to E-mail: yangzhang31@126.com; swang@utk.edu

Meanwhile, there are abundant researches about nanocellulose, which was referred also as crystals or fibers in nano-level and whiskers, and the study is mostly engaged in the general isolation, the way for its characterization, and extensive use of cellulose in various areas [9]. Lately, the interest in nanocellulose has sharply increased due to its specific chemical and physical properties [10]. The representative of third generation of novel materials cellulose aerogels retains the advantages of traditional aerogels, such as lightweight, high porosity and high specific surface area [11, 12], exhibiting its own unique advantages, including high availability of raw materials, and biocompatibility [9]. In addition, its unique porous structural features render it potential candidates for various energy and environmental applications, e.g., energy storage, gas sensing, drug delivery and adsorbent materials [13].

The recent advances in cellulose functional materials [14], nanocellulose [15], as well as on the surface modification of cellulosic materials [16] have been reviewed. It has been clearly shown that the cellulose possess a lot of functional groups separately such as carboxylic, hydroxyl, methoxy, and phenolic groups [9]. The special component enables cellulose-based materials to be employed in various processes, offering the potential of different chemical modifications due to the abundance of hydroxyl groups on the surface of cellulose [3]. One of the main modification methods is the direct modification, where the functional groups can attach to hydroxyl groups of cellulose via a variety of chemical processes [3, 9]. The esterification [17], etherification [14], oxidation [18], alkali treatment [19] and silynation [20] are the common methods for cellulose modification to prepare adsorbent materials.

Since aminosilane is a well-known compound for carbon dioxide (CO_2) capture, whereas cellulose nanocrystal (CNC) acts as a based material for N-(2-aminoethyl)(3-aminopropyl) methyldimethoxysilane (AEAPMDS) grafting, it is of worth investigating the particular characteristics of this system.

In this work, we prepared the CNC using microcrystalline cellulose (MCC) as a raw material by the acid hydrolysis method. The modification of CNC by AEAPMDS was in turn carried out in order to obtain spherical amino-modified AEAPMDS-CNC nanocellulose hydrogel. Finally, the AEAPMDS-CNC spherical aerogels were prepared via freeze-drying or supercritical CO_2 drying technology in combination

with solvent exchange and its biophysical properties were evaluated.

Materials and methods

Materials

Microcrystalline cellulose (MCC; 50 μm in size) was purchased from Anhui Sunvo Medicinal Materials Co., Ltd (Hefei, China). N-(2-aminoethyl)-3-amino-propylmethyldimethoxysilane (AEAPDMS, 97% purity) was supplied from Alfa Aesar (United Kingdom) and used as received. All chemicals were of analytical grade and used without further purification. Sulfuric acid (98%), Tert-butyl alcohol (99.7%), ethanol (99.7%), and calcium chloride were purchased from China Sinopharm Chemical Reagent Co., Ltd. (analytical grade, Shanghai, China). Dialysis membranes ($\cong$ 14,000 Da, 3 in. width, MWCO: 8000–14,000) was purchased from Union Carbide Corporation.

CNC production

MCC was hydrolyzed by sulfuric acid into cellulose nanocrystals (CNC). In brief, MCC (10 g) was mixed with 63% H_2SO_4 solution at 1:10 ratio (m/v), agitating for 1 h at 45 °C, then 500 mL distilled water was added. The obtained solution is supposed to stop dialyzation when its pH became 7.0, and sonicated about half an hour in a cell smash with ultrasound (XO-2500D, Nanjing Xianou Instrument Manufacturing Co., Ltd., Nanjing, China.) with a constant power of 2000 W [11, 13].

Preparation of spherical amine-modified nanocellulose aerogel

The preparation of amine-modified nanocellulose aerogels was scheduled as shown in Fig. 1. The CNC was firstly dissolved in distilled water and treated in an ultrasonic cell smash with a constant power of 2000 W for 5 min to form a homogeneous solution of 2.5 wt%. AEAPMDS was added to this CNC hydrogel until the total silane concentration was 4 wt%. The suspension was sonicated for 45 s, followed by a spontaneous physical gelation route for 20 min at room temperature. The colloid was slowly dropped (each drop is about 0.2 mL) into 40 mL of 0.25 mol/L

Figure 1 Flow chart for preparation of AEAPMDS nanocellulose aerogels.
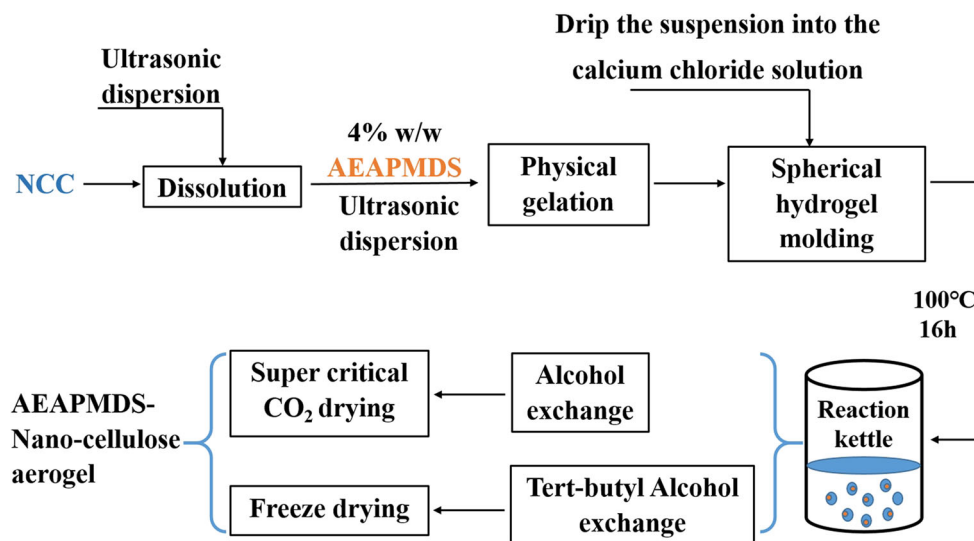
calcium chloride solution with a syringe towards the formation of wet spherical amino-modified AEAPMDS-CNC nanocellulose aerogel by the physical gelation in charge of calcium ion. Then, the prepared spherical CNC/AEAPMDS hydrogels were added into a reaction kettle, containing ethanol with a solid to liquid ratio of 1:10 at 100 °C and reacted for 16hs. Finally, calcium chloride solution was replaced with tert-butyl alcohol and ethanol in different percentages (25, 50, 75 and 100%). Freeze-drying and supercritical CO_2 drying were carried out by an extraction autoclave with a pressure of 120 bar and a temperature of 40 °C using pure carbon dioxide (SET-150). The resulting materials were referred to as FD-AEAPMDS-CNC aerogel and SD-AEAPMDS-CNC aerogel. For comparison purposes, the above synthesis procedure was repeated without silane and the produced sample was designated as CNC aerogel.

Measurement of shrinkage

Measurement of shrinkage was performed as previously described [11]. Drying shrinkage was calculated by the following formula: $S = (L_0 - L_C)/L_0 \times 100\%$, where S, L_0, and L_C are shrinkage, longest aerogel diameter obtained before and after drying, respectively. More than 50 balls were measured to count the average size.

Fourier transform infrared spectroscopy (FTIR)

The chemical structure of the CNCs was obtained by means of Fourier transform infrared spectroscopy (FTIR) in a Nicolet380 FTIR-ATR spectrometer (Spectrum One, Thermo Fisher Scientific, USA) as previously described [21]. Data were collected from 600 to 4000 cm^{-1} at a resolution of 4 cm^{-1}, and an average of 100 scans was collected for each spectrum. Each sample was tested in triplicate.

X-ray diffraction (XRD)

To determine the crystalline structure of the CNC, XRD measurements were performed on an Ultima IV multipurpose X-ray diffraction system (X'TRA, ARL, Switzerland). The diffracted intensity of Cu Kα radiation (wavelength, λ = 0.1542 nm; 40 kV and 30 mA) was measured in a 2θ range between 10° and 50°. Multiple scans were undertaken on each sample. The crystallinity index (CI) was calculated from the height ratio between the intensity of the crystalline region (I002 at 2θ = 22.5°) and the intensity of the amorphous region (Iam at 2θ = 18.5°) using the Segal method [22].

Solid-state ^{13}C CP/MAS NMR characterization

The solid-state ^{13}C cross-polarization magic angle spinning nuclear magnetic resonance (CP/MAS-NMR) spectra of the CNC were recorded at room

temperature, using a 4 mm CP/MAS probe on a Bruker AVIII 400 MHz WB spectrometer (Bruker Inc., Germany) at a ^{13}C frequency of 100.62 MHz. CP/MAS experiments utilized 10 kHz MAS probe head spinning speed, 1.8 ms contact pulse, 2 s recycle delay and appropriate numbers of scans to yield reasonable signal-to-noise ratios [23].

N$_2$ sorption isotherms

Nitrogen adsorption–desorption isotherms were obtained using a surface area and pore size analyzer (ASAP 2020 Analyzer Micromeritics, USA). Before measurements, the nanocellulose aerogels were placed in vacuum overnight. The specific surface area was determined by N$_2$ adsorption (Belsorb) through the Brunauer–Emmet–Teller (BET) equation. Approximately, 40 mg of the aerogels samples was dried in a vacuum oven. The nitrogen adsorption was measured at 77 K.

Morphological characterization

Micromorphological features of the nanocellulose aerogels were observed using a scanning electron microscope (SEM; Zeiss Auriga SEM/FIB crossbeam workstation, Germany; JSM-7600, JEOL, Japan). Thin layers of gold were deposited by sputtering with scan-coat onto the surface of the cross-sections to avoid build up of electrostatic charge.

Thermogravimetric analysis (TGA)

Thermal stability was determined using a thermal gravimetric analyzer (TGA, Perkin-Elmer 7 series, Perkin-Elmer Cetus Instruments, Norwalk, CT, USA). The temperature was raised from 35 to 600 °C at a heating rate of 10 °C/min. The curve of Differential Thermal Gravity (DTG) was derived by the first-order differential of the TG curve. Each sample was tested in triplicate. [24].

Elemental analysis

The elemental analysis was used to determine whether the modifier was successfully grafted onto the CNC as well as to investigate the impact of different parameters (temperature, time, modifier) on the modification process. The nitrogen content of AEAPMDS-CNC was obtained through elemental analysis (Elemental Analyzer, Vario EL III, Elementar, Germany).

Statistical analysis

Continuous data are shown as the mean ± standard deviation (SD) with three independent tests, and were analyzed using SPSS 17 (SPSS, Chicago, IL, USA). $P < 0.05$ was considered as significant difference.

Results and discussion

Analysis of FTIR

The FTIR spectra of CNC and AEAPMDS-CNC are shown in Fig. 2a. Both the spectrums of CNC and AEAPMDS-CNC exhibited typical bands for cellulose. Such as the wide absorption band at 3341 cm^{-1}, related to aromatic and aliphatic –OH groups, and the bands at 2900 and 1425 cm^{-1} attributed to the C–H vibration of –CH$_2$ and –CH$_3$ groups, respectively [25–27]. The CH$_2$ symmetric bending appeared at 1428 cm^{-1}, whereas the –OH and –CH bending, C–C and C–O [25] stretching appeared at 1372, 1316 and 1116 cm^{-1}, respectively. The band at 1162 cm^{-1} was assigned to C–O–C asymmetric stretching vibration from the glycosidic ring, whereas the band at 1058 cm^{-1} was attributed to C–O symmetric stretching. The band at 896 and 667 cm^{-1} are attributed to the CH out-plane bending and OH out-plane bending, respectively [16, 26]. These results indicated that the amine-modified aerogel still retained the internal structure of cellulose after the modification and heating processes [12]. In addition to FTIR spectra, X-ray diffraction measurements also confirm that amine-modified CNC still maintains the structure of native cellulose, called cellulose I (Fig. 2b). Moreover, the CrI of modified NCC was reduced due to the amorphous AEAPDMS after amine-modified reaction, indicating that AEAPDMS was grafted onto NCC via silanization [2].

Moreover, in Fig. 2a, a strong absorption peak at 1639 cm^{-1} in CNC sample is appeared, which is related to the O–H bending vibration of water absorbed by the cellulose [25]. In contrast, this absorption peak was very weak in the AEAPMDS CNC, implying a less hydrophilic nature of modified aerogels as compared to the unmodified ones [27]. In
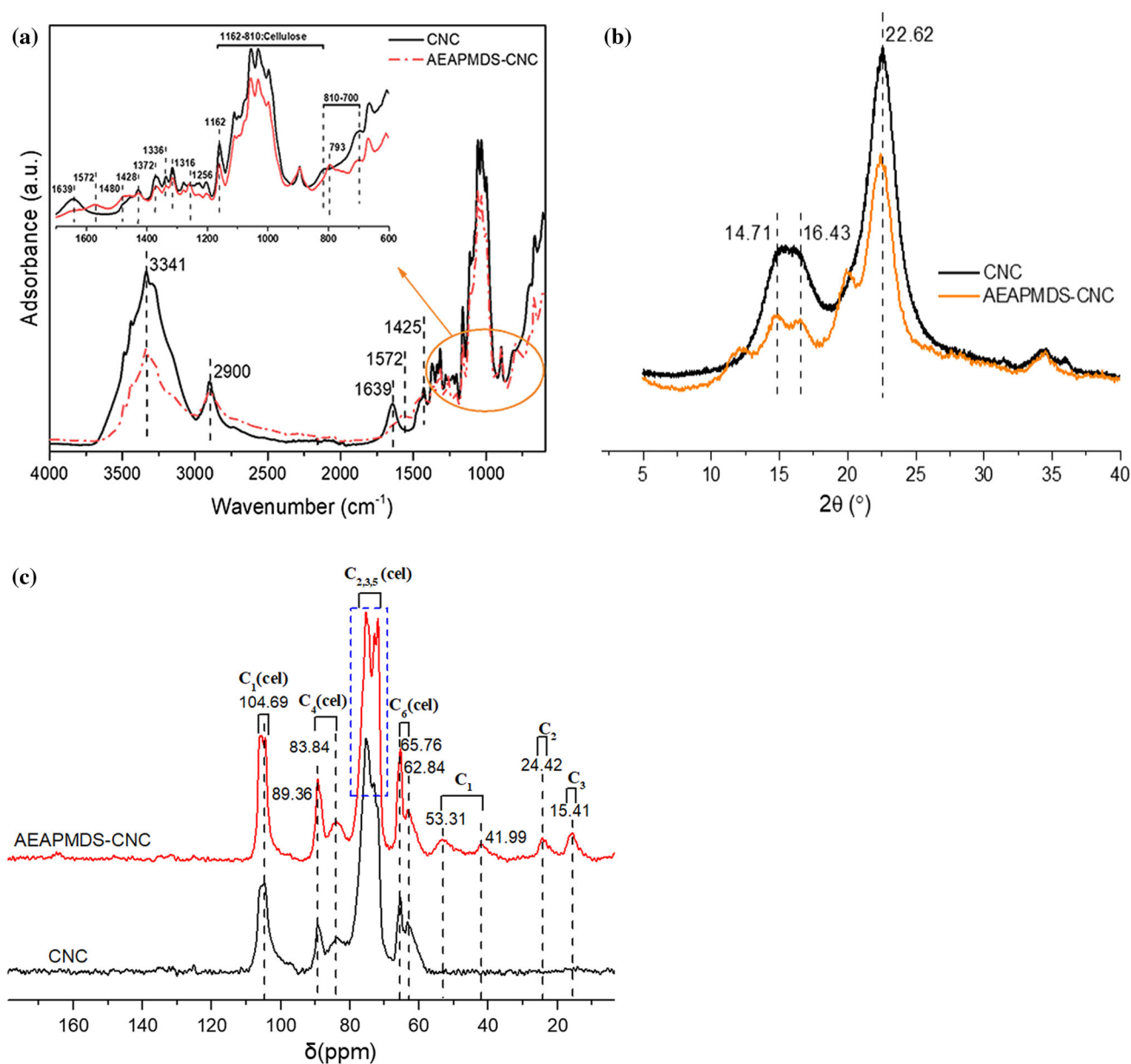
Figure 2 **a** The FTIR spectra of CNC and AEAPMDS-CNC in the following wave number range: full range: 4000–600, and 1700–600 cm^{-1}. **b** The XRD spectra of CNC and AEAPMDS-CNC. **c** ^{13}C CP/MAS NMR spectrum of CNC and AEAPMDS-CNC.

addition, some new peaks appeared in the spectrum of modified AEAPMDS-CNC sample. As compared with the unmodified CNC sample, i.e.: the N–H bending of the NH$_2$ group at 1572 and 1480 cm^{-1}, the C–N stretching vibration peak at 1336 cm^{-1}, the Si–C stretching vibration peak at ca. 1256 cm^{-1}, the stretching vibration peak of Si–O–cellulose at ca. 1033 cm^{-1} and the Si–O–Si stretching vibration peak at 793 cm^{-1} [12, 28, 29].

Analysis of NMR

Then, the structural features of nanocellulose and amine-modified nanocellulose were further investigated by solid-state NMR. In Fig. 2c, the ^{13}C NMR spectrum of unmodified CNC is depicted. The typical signals of cellulose were assigned to C1 (104.69 ppm), C4 crystalline (89.36 ppm), C4 amorphous (83.84 ppm), C2/C3/C5 (75.36 and 71.36 ppm), C6 crystalline (65.76 ppm), and C6 amorphous (62.84 ppm) resonance signals [23, 30]. The six

characteristic signals in the range of 60–120 ppm, assigned to carbon resonances of cellulose framework, were also appeared in the ^{13}C NMR spectrum of AEAPMDS-CNC. However, no shifting of these signals was observed as compared to bare CNC, whereas the intensity of C2/C3/C5 and C6 signals was increased. In addition, four signals of low intensity were observed at 15.41, 24.42, 41.99 and 53.31 ppm assigned to the carbon resonances in the –Si–C(3)H$_2$–, –C(2)H$_2$– and –C(1)H$_2$–NH$_2$– groups, respectively, of the AEAPMDS [30, 31]. These findings suggest that the chemical structure of cellulose is maintained, indicating the successful grafting of the AEAPMDS into CNC. The proposed modification mechanism is described in Fig. 3.

N$_2$ sorption isotherms

The nitrogen adsorption/desorption isotherms and the corresponding BJH pore size distributions of the CNC aerogel and AEAPMDS-CNC aerogel are shown in Fig. 4. According to the classification of IUPAC (International Union of Pure and Applied Chemistry), all the cellulose aerogels with such preparation displayed showed type IV hysteresis between the adsorption and desorption branches, indicating the existence of mesopores in the as-prepared aerogels. In the low pressure region, the curves exhibit a rounded knee implying monolayer adsorption with minor micropores. In the middle pressure range, the rapid increase of nitrogen adsorption
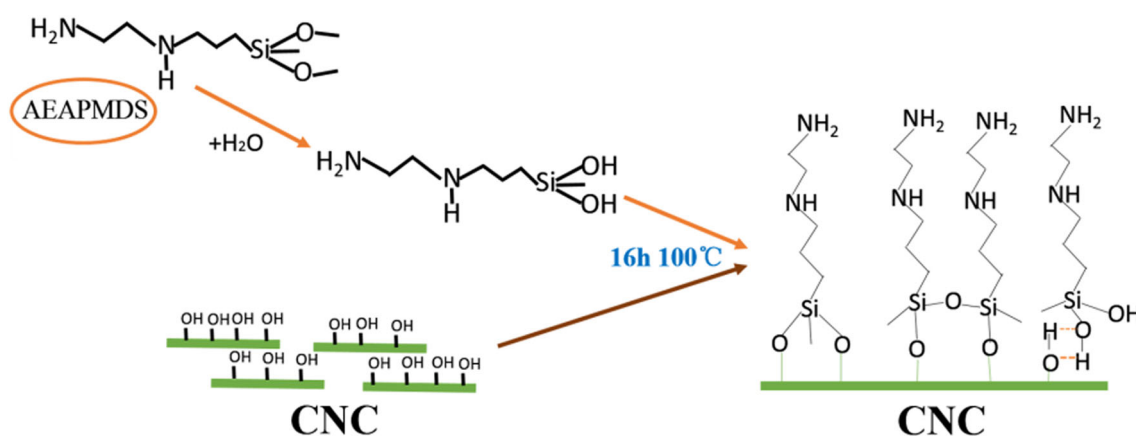

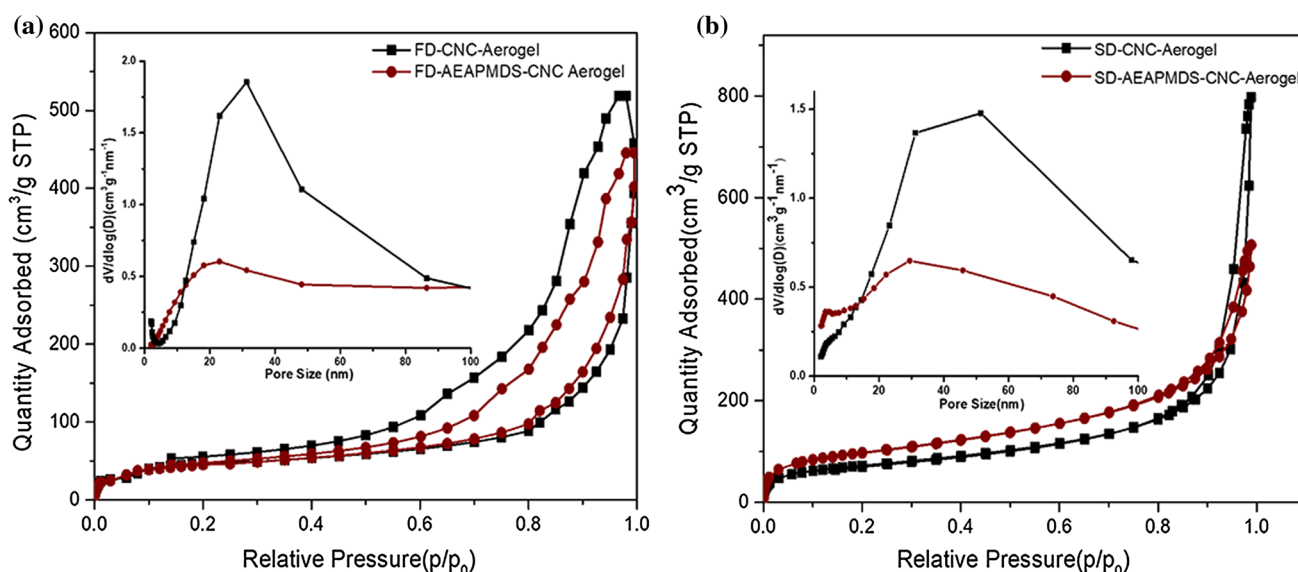Figure 3 Schematic diagram of modification mechanism on CNC by AEAPMDS.

Figure 4 a N$_2$ sorption isotherms at 77 K and pore size distributions of the CNC aerogel and AEAPMDS-CNC aerogel by freeze drying. b N$_2$ sorption isotherms at 77 K and pore size distributions of the CNC aerogel and AEAPMDS-CNC aerogel by supercritical CO$_2$ drying.

Table 1 Specific surface area, pore volume, average pore size and shrinkage of the nanocellulose aerogels

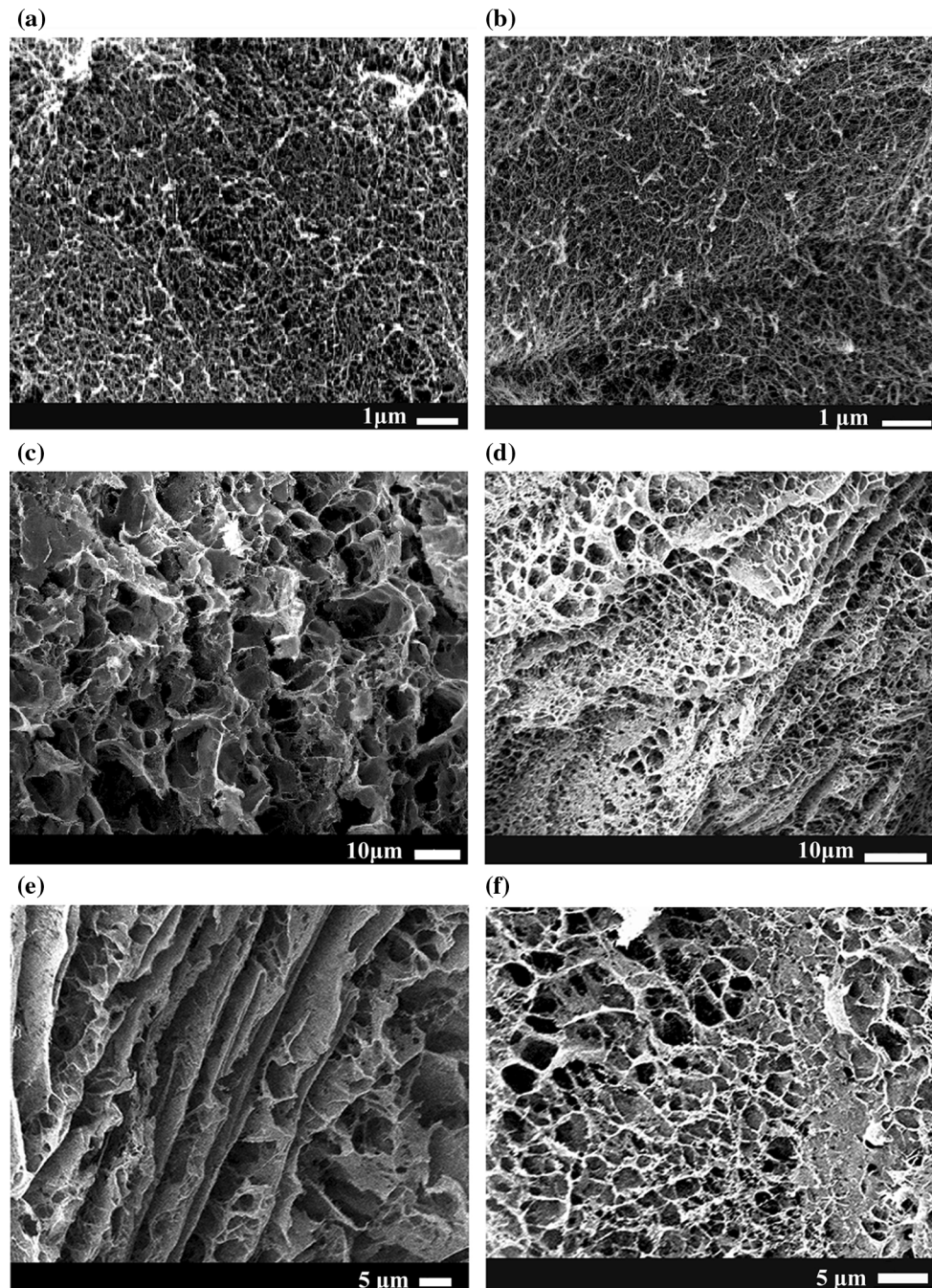| Sample	S_{BET} (m²/g)	V_g (cm³/g)	Average pore size (nm)	Shrinkage (%)
SD-CNC aerogel	353.8	0.783	8.86	4.03
SD-AEAPMDS/CNC aerogel	262.0	1.076	10.4	4.53
FD-CNC aerogel	165.3	0.689	16.7	7.85
FD-AEAPMDS/CNC aerogel	120.4	0.471	17.7	8.12

Figure 5 SEM images of prepared CNC aerogel and AEAPMDS-CNC aerogel. **a** CNC aerogel prepared by supercritical CO₂ drying. **b** AEAPMDS-CNC aerogel prepared by supercritical CO₂ drying. **c** CNC aerogel prepared by freeze drying. **d–f** AEAPMDS-CNC aerogel prepared by freeze drying.
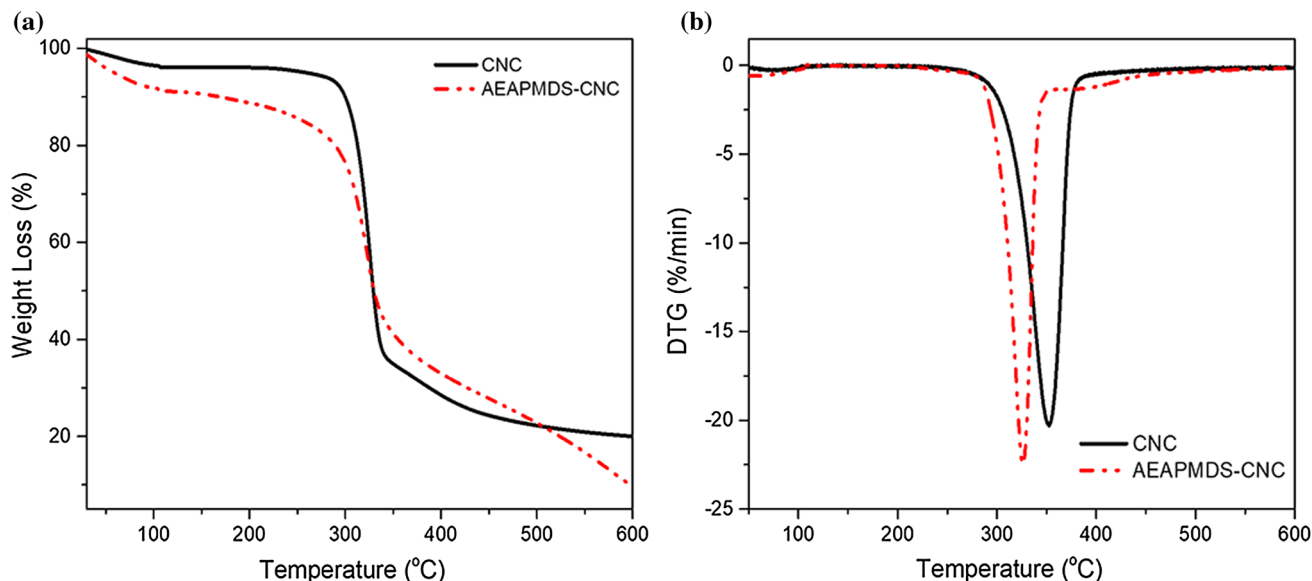
Figure 6 TG (**a**) and DTG (**b**) curves of the CNC and AEAPMDS-CNC.

quantity and the low slope region in the middle of isotherms indicated the existence of multilayer adsorption with Type-III hysteresis (IUPAC classification). The latter implies capillary condensation of the meso and macropores of slit-like shape. Table 1 displays the results of the specific surface area, pore volume, pore size and density at average. Compared with the CNC aerogel, the specific surface area was reduced by AEAPMDS modification. However, the uniformity of the pores and the internal structure is improved in AEAPMDS-CNC aerogel. Furthermore, the pore size distribution was consistent with the nitrogen physisorption isotherms and the morphological characteristics (SEM).

Surface morphology

Figure 5 shows representative SEM images of CNC and amine-modified CNC samples prepared by supercritical drying and freeze drying. As shown in Fig. S1, the addition of modifier had nearly no obvious influence on the shape of the spherical nanocellulose aerogels [12]. On the other hand, the CNC aerogel has turned from white at first into pale yellow in the end. Both the CNC aerogel and AEAPMDS-CNC aerogel dried by freeze-drying displayed a porous network consisting of film-like structures, which seemed to be caused by the aggregation of nanocellulose whiskers during freeze drying. Simultaneously, the CNC aerogel and AEAPMDS-CNC aerogel prepared by supercritical CO_2 drying

exhibited a three-dimensional nano-structured network which is composed of irregularly arranged nanofibrils due to the hydrogen bonding between the CNC hydroxyl groups. The rod-like shape nanofibrils have a mean diameter of 25.4 ± 5 nm (range 10–45 nm) (Fig. S2), with a length to diameter ratio in the range of 11–18. From the images in Fig. 5a, b, it can be seen that all the aerogels were highly porous, showing that the pore morphology did not collapse during processing, and a highly porous structure was maintained. The latter is consistent with the textural characteristics of the samples, previously analyzed. Moreover, compared with the unmodified CNC aerogel, the internal structure of AEAPMDS-CNC seems like a honeycomb comprised of squares, polygons and circles as appeared in Fig. 5c, d. In Fig. 5e, f the structure of FD-AEAPMDS-CNC aerogel is shown. The tunnel-like structure is supposed to be influenced by the condensation of the fibrils when the material is frozen (Fig. 5e), while the honeycomb structure comprising squares, polygons and circles is more obvious. This latter clearly implies that AEAPMDS accessed the CNC successfully having a great influence in the network structure of the CNC aerogels.

In the present work, both supercritical CO_2 drying and freeze-drying were employed as drying methods. As previously demonstrated [32], the supercritical drying technique offers unique advantages in terms of high pore texture and low shrinkage.
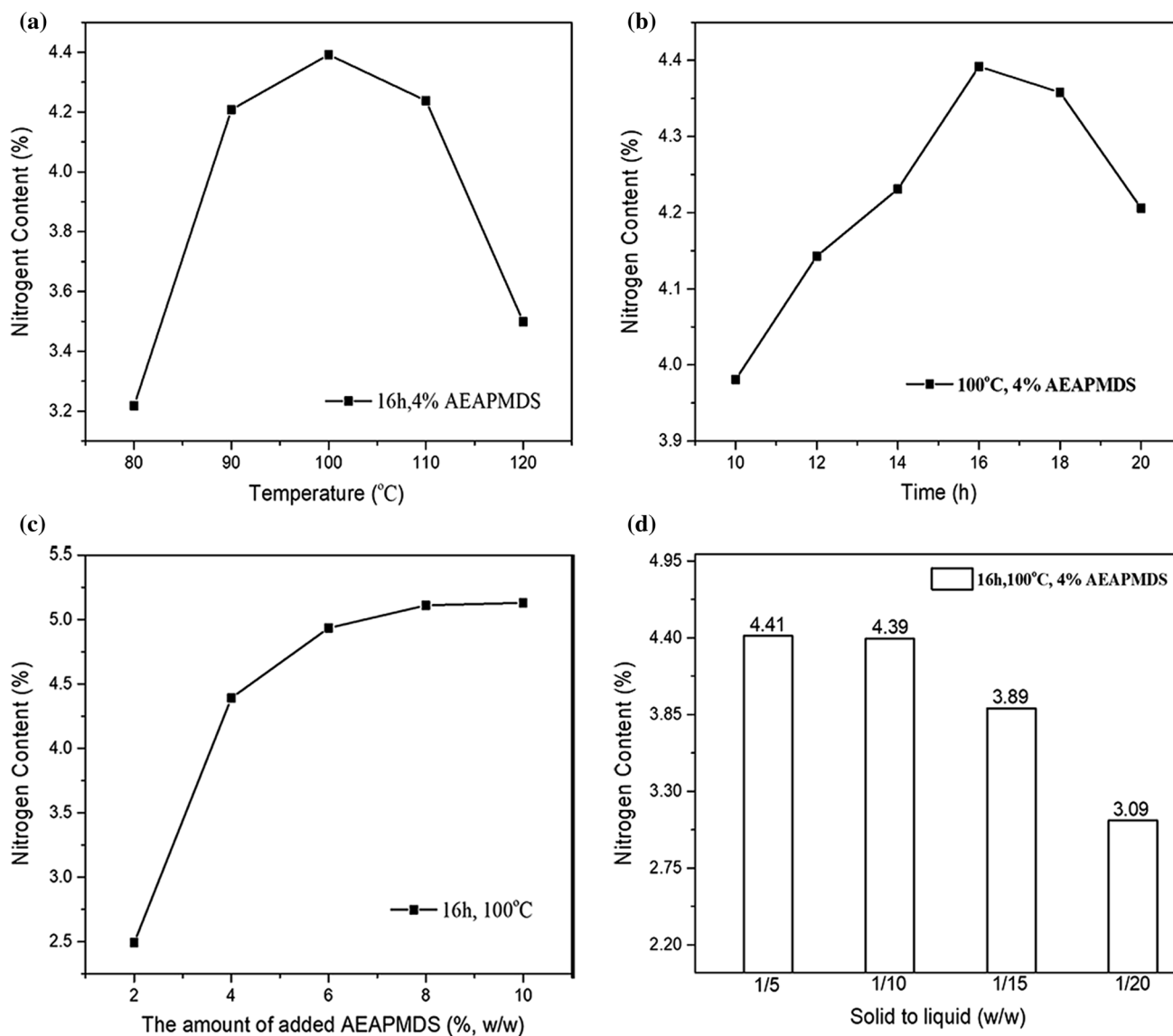
Figure 7 Effect of reaction temperature, time, the amount of added AEAPMDS and solid to liquid ratio on N% of AEAPMDS-CNC. **a** Reaction temperature. **b** Reaction time. **c** AEAPMDS amount. **d** Solid to liquid ratio.

However, this technique cannot be easily applied at industrial scale due to the need of special equipment, liquid carbon dioxide, and in consequence higher cost. Herein, a facile process, i.e., freeze-drying combined with tert-butyl alcohol solvent, was employed towards the synthesis of aerogels with a honeycomb structure comprising squares, polygons and circles. Tert-butanol solvent can lead to improved textural properties, since it prevents the damage of gel network and the shrinkage of aerogels during the drying process [33].

Thermal stability

Thermogravimetric analysis was conducted to investigate the differences in the thermal decomposition properties of CNC and AEAPMDS-CNC. The weight loss curves are plotted in Fig. 6. The tunnel-like structure is supposed to be influenced by the condensation of the fibrils when the material is frozen. In the chart, we can find that there is a thermal degradation between 200 and 400 °C, and it may be linked to disruption of cellulose glycosidic linkages [34]. Meanwhile, the temperature of the maximum weight loss rate (T_{max}) of unmodified CNC is higher

than that of the modified AEAPMDS-CNC, implying a different thermal stability and successful modification upon the amination process.

Effect of preparation conditions on nitrogen content

The effect of different reaction parameters (temperature, time, AEAPMDS amount, solid to liquid ratio) on the nitrogen content of AEAPMDS-CNC was subsequently investigated in order to gain insight into the underlying mechanism of CNC modification by amines (in Fig. 7).

As can be seen from Fig. 7a, b, the nitrogen content was initially increased in AEAPMDS-CNC upon increasing time and temperature, followed, however, by a substantial decrease at high temperatures and prolonged time. The reason of this volcano behavior is not clear, and it may be related to the formation of amino silanol by methoxy hydrolysis in AEAPMDS at the beginning stages. In this regard, it was revealed that upon heating conditions, the hydroxyl groups of AEAPMDS and the surface of nanocellulose were condensed, accompanied by the loss of a water molecule and the formation of modified nanocellulose by amino silane [9, 20]. In fact, since this particular reaction is reversible, the reduction of water in the hydrogel could influent the hydrolysis rate at temperatures higher than 100 °C. At the same time, the modifier in CNC may be dispersed into ethanol at high temperatures. Under the present conditions, we observed that the appropriate time and temperature were 16 h and 100 °C, respectively. Regarding the impact of AEAPMDS, it was observed that nitrogen content is proportional to the amount of AEAPMDS (Fig. 7c) without, however, following a linear trend. The latter can be ascribed to the limited number of hydrogen groups which progressively consumed by AEAPMDS, resulted finally to a steady state (plateau in Fig. 7c). Finally, Fig. 7d shows that nitrogen content was progressively decreased with increasing ethanol, i.e., decreasing the solid-to-liquid ratio. These results showed that the time and temperature modification, solid-to-liquid ratio and the amount of AEAPMDS added to nanocellulose had a certain effect on the nitrogen content. The optimum reaction conditions were identified as follows: reaction time of 16 h, reaction temperature of 100 °C and solid-to-liquid ratio (w/w) of 1:10. Based on these optimum values, about 4% of the amount of AEAPMDS consumption can be effectively saved.

Conclusions

In this study, the synthesis of amine functionalized nanofibrillated cellulose is experimentally investigated. The reaction conditions relevant to the modification of CNC by AEAPMDS were systematically explored and the AEAPMDS-CNC aerogel was successfully prepared by freeze-drying technology and supercritical CO_2 drying in combination with solvent exchange. AEAPMDS was successfully grafted onto CNC as clearly revealed by the different characterization studies. The as-prepared AEAPMDS-CNC aerogels exhibit a low shrinkage rate and high specific surface areas. They exhibited a 3D nanostructured network which is composed of irregularly arranged nanofibrils via supercritical drying technology while tert-butyl alcohol aids in the formation of directional honeycomb structure when it is undergoing the freeze-drying owing to the lower surface tension. This work demonstrates the potential of amination to functionalize spherical CNC aerogels, offering new opportunities for the design of novel functional biomaterials with controlled properties.

Acknowledgements

Electronic supplementary material: The online version of this article (https://doi.org/10.1007/s10853-018-2595-7) contains supplementary material, which is available to authorized users.

References

[1] Chirayil CJ, Mathew L, Thomas S (2013) Review of recent research in nanocellulose preparation from different ligni-cellulosic fibers. Rev Adv Mater Sci 37:20–28

[2] Mohd NH, Arman Alim AA, Zahari JI et al (2017) Properties of aminosilane modified nanocrytalline cellulose (NCC) from oil palm empty fruit bunch (OPEFB) fibers. Mater Sci Forum 88:284–289

[3] Kang H, Liu R, Huang Y (2015) Graft modification of cellulose: methods, properties and applications. Polymer 70:A1–A16

[4] Sani A, Dahman Y (2010) Improvements in the production of bacterial synthesized biocellulose nanofibres using different culture methods. J Chem Technol Biotechnol 85:151–164

[5] Yu H, Liu R, Qiu L, Huang Y (2007) Composition of the cell wall in the stem and leaf sheath of wheat straw. J Appl Polym Sci 104:1236–1240

[6] Fu J, Wang S, He C, Lu Z, Huang J, Chen Z (2016) Facilitated fabrication of high strength silica aerogels using cellulose nanofibrils as scaffold. Carbohydr Polym 147:89–96

[7] Sun H, Miao J, Yu Y, Zhang L (2015) Dissolution of cellulose with a novel solvent and formation of regenerated cellulose fiber. Appl Phys A-Mater 119:539–546

[8] Huang H, Chen X, Yuan W (2006) Microencapsulation based on emulsification for producing pharmaceutical products: a literature review. Dev Chem Eng Mineral Process 14:515–544

[9] Hokkanen S, Bhatnagar A, Sillanpaa M (2016) A review on modification methods to cellulose-based adsorbents to improve adsorption capacity. Water Res 91:156–173

[10] Nechyporchuk O, Belgacem MN, Bras J (2016) Production of cellulose nanofibrils: a review of recent advances. Ind Crop Prod 93:2–25

[11] Wang X, Zhang Y, Jiang H, Song Y, Zhou Z, Zhao H (2016) Fabrication and characterization of nano-cellulose aerogels via supercritical CO_2 drying technology. Mater Lett 183:179–182

[12] Liu S, Zhang Y, Jiang H, Wang X, Zhang T, Yao Y (2018) High CO2 adsorption by amino-modified bio-spherical cellulose nanofibres aerogels. Environ Chem Lett 16:605–614

[13] Wang X, Zhang Y, Jiang H, Song Y, Zhou Z, Zhao H (2017) Tert-butyl alcohol used to fabricate nano-cellulose aerogels via freeze-drying technology. Mater Res Express 4:065006. https://doi.org/10.1088/2053-1591/aa72bc

[14] Fox SC, Li B, Xu D, Edgar KJ (2011) Regioselective esterification and etherification of cellulose: a review. Biomacromolecules 12:1956–1972

[15] Lavoine N, Desloges I, Dufresne A, Bras J (2012) Microfibrillated cellulose - its barrier properties and applications in cellulosic materials: a review. Carbohydr Polym 90:735–764

[16] J-i Kadokawa (2016) Dissolution, gelation, functionalization, and material preparation of chitin using ionic liquids. Pure Appl Chem 88:621–629

[17] Batmaz R, Mohammed N, Zaman M, Minhas G, Berry RM, Tam KC (2014) Cellulose nanocrystals as promising adsorbents for the removal of cationic dyes. Cellulose 21:1655–1665

[18] Saito T, Isogai A (2005) Ion-exchange behavior of carboxylate groups in fibrous cellulose oxidized by the TEMPO-mediated system. Carbohydr Polym 61:183–190

[19] Memon SQ, Memon N, Shah SW, Khuhawar MY, Bhanger MI (2007) Sawdust—a green and economical sorbent for the removal of cadmium (II) ions. J Hazard Mater 139:116–121

[20] Xie Y, Hill CAS, Xiao Z, Militz H, Mai C (2010) Silane coupling agents used for natural fiber/polymer composites: a review. Compos Part A Appl Sci Manuf 41:806–819

[21] Qua EH, Hornsby PR, Sharma HSS, Lyons G (2011) Preparation and characterisation of cellulose nanofibres. J Mater Sci 46:6029–6045. https://doi.org/10.1007/s10853-011-5565-x

[22] Park S, Baker JO, Himmel ME, Parilla PA, Johnson DK (2010) Cellulose crystallinity index: measurement techniques and their impact on interpreting cellulase performance. Biotechnol Biofuels 3:10. https://doi.org/10.1186/1754-6834-3-10

[23] Zhang Z, Sèbe G, Rentsch D, Zimmermann T, Tingaut P (2014) Ultralightweight and flexible silylated nanocellulose sponges for the selective removal of oil from water. Chem Mater 26:2659–2668

[24] Ren S, Zhang X, Dong L et al (2017) Cellulose nanocrystal supported superparamagnetic nanorods with aminated silica shell: synthesis and properties. J Mater Sci 52:6432–6441. https://doi.org/10.1007/s10853-017-0878-z

[25] Gebald C, Wurzbacher JA, Tingaut P, Zimmermann T, Steinfeld A (2011) Amine-based nanofibrillated cellulose as adsorbent for CO_2 capture from air. Environ Sci Technol 45:9101–9108

[26] Gebald C, Wurzbacher JA, Tingaut P, Steinfeld A (2013) Stability of amine-functionalized cellulose during temperature-vacuum-swing cycling for CO_2 capture from air. Environ Sci Technol 47:10063–10070

[27] Gebald C, Wurzbacher JA, Borgschulte A, Zimmermann T, Steinfeld A (2014) Single-component and binary CO_2 and H_2O adsorption of amine-functionalized cellulose. Environ Sci Technol 48:2497–2504

[28] Lu J, Askeland P, Drzal LT (2008) Surface modification of microfibrillated cellulose for epoxy composite applications. Polymer 49:1285–1296

[29] Abdelmouleh M, Boufi S, Belgacem MN, Duarte AP, Ben Salah A, Gandini A (2004) Modification of cellulosic fibres with functionalised silanes: development of surface properties. Int J Adhes Adhes 24:43–54

[30] Gamelas JAF, Oliveira F, Evtyugina MG, Portugal I, Evtuguin DV (2016) Catalytic oxidation of formaldehyde by ruthenium multisubstitutedtungstosilicic polyoxometalate supported on cellulose/silica hybrid. Appl Catal A Gen 509:8–16

[31] Gamelas JAF, Evtuguin DV, Esculcas AP (2007) Transition metal substituted polyoxometalates supported on amine-functionalized silica. Trans Metal Chem 32:1061–1067

[32] Pekala RW (1989) Organic aerogels from the polycondensation of resorcinol with formaldehyde. J Mater Sci 24:3221–3227. https://doi.org/10.1007/BF01139044

[33] Job N, Théry A, Pirard R et al (2005) Carbon aerogels, cryogels and xerogels: influence of the drying method on the textural properties of porous carbon materials. Carbon 43:2481–2494

[34] Lee KY, Tammelin T, Schulfter K, Kiiskinen H, Samela J, Bismarck A (2012) High performance cellulose nanocomposites: comparing the reinforcing ability of bacterial cellulose and nanofibrillated cellulose. ACS Appl Mater Interfaces 4:4078–4086